

- with the performance of ten cytotechnologists found that the distinction between abnormal and normal cells was made with $A = 0.90$ by the computer and $A = 0.87$ by the cytotechnologists (32). The classical studies of "observer error" in radiology were made for chest films in the diagnosis of tuberculosis, and were conducted by Garland and by Yerushalmy and associates in the late 1940s [L. H. Garland, *Radiology* 52, 309 (1949); J. Yerushalmy, J. T. Harkness, J. H. Cope, B. R. Kennedy, *Am. Rev. Tuberculosis* 61, 443 (1950)]. They were reanalyzed in ROC terms by Lusted in his book (33), which introduced students of medical decision-making to the ROC. Although the data points from the two studies were in different portions of the ROC graph, for both studies $A = 0.98$. (Meanwhile, values of "percentage correct" for the two studies are 83 and 91%, indicating, spuriously, a difference in accuracy.) One recent study of chest films (34) gave A values of 0.94 and 0.91 for the detection of two specific abnormalities (pneumothoraces and interstitial infiltrates). Another, with diverse lesions, showed $A = 0.79$ when the observer was not prompted by the case history and 0.88 when he or she was (35).
29. R. L. Egan, *Mammography* (Thomas, Springfield, IL, 1964).
 30. J. E. Gohagan et al., *Invest. Radiol.* 19, 587 (1984).
 31. J. E. Goin, J. D. Haberman, M. K. Linder, P. A. Lambird, *Radiology* 148, 393 (1983).
 32. J. W. Bacus, *Application of Digital Image Processing Techniques to Cytology Automation* (Technical Report, Rush Presbyterian-St. Luke's Medical Center, Medical Automation Research Unit, Chicago, 1982). Some results of this study were reported by J. W. Bacus et al., *Anal. Quant. Cytol. Histol.* 6, 121 (1984).
 33. L. B. Lusted, *Introduction to Medical Decision Making* (Thomas, Springfield, IL, 1968).
 34. H. MacMahon et al., *Radiology* 158, 21 (1986).
 35. K. S. Berbaum et al., *Invest. Radiol.* 21, 532 (1986).
 36. J. A. Swets, *Mater. Eval.* 41, 1294 (1983).
 37. G. Ben-Shakhar, I. Lieblich, Y. Bar-Hillel, *J. Appl. Psychol.* 67, 701 (1986).
 38. L. Saxe, D. Dougherty, B. Scott, *Am. Psychol.* 40, 794 (1985).
 39. J. J. Szucko and B. Kleinmuntz, *ibid.* 36, 488 (1981).
 40. R. Gray, C. B. Begg, R. A. Greenes, *Med. Decis. Making* 4, 151 (1984).
 41. A review of the polygraph assessment literature, which treats the problems mentioned here and some more specific, concludes that measured accuracy values are likely to be inflated by a wide margin (37). That inflation is even more marked when a measurement of "percentage of correct decisions" is made rather than a measurement of A . That percentage measure sets aside cases having polygraph records that the examiner deems inconclusive—in effect, cases on which he or she chooses not to be scored.
 42. I should observe in passing that accuracy measures may be biased by certain general factors other than the four treated here. The one that comes first to mind is that system tests are often conducted under laboratory, rather than field, conditions. Thus, radiologists may participate in laboratory tests under unusually good conditions: quiet, no interruptions, and no patient treatment depending on the diagnosis. Such a test may be conducted purposely, in order to test a system in a standard way and at its full potential, but the measured value may be higher than can be expected in practice.
 43. Since the concern for evaluation in the field of information retrieval heightened in the 1950s, this field has used several different measures of accuracy intended to be independent of the decision criterion; see, for example, a review by J. A. Swets, *Science* 141, 245 (1963). ROC measures have been considered extensively, for example, by B. C. Brookes, *J. Doc.* 24, 41 (1968); M. H. Heine, *ibid.* 29, 81 (1973); A. Bookstein, *Recall Precision* 30, 374 (1974); M. H. Heine, *J. Doc.* 31, 283 (1975); M. Kochen, Ed., *The Growth of Knowledge* (Wiley, New York, 1967); T. Saracevic, Ed., *Introduction to Information Science* (Bowker, New York, 1970); B. Griffith, Ed., *Key Papers in Information Science* (Knowledge Industry Publications, White Plains, NY, 1980).
 44. Various scores for binary forecasts that were developed in this field were related to ROC measures by I. Mason, in *Ninth Conference on Weather Forecasting and Analysis* (American Meteorological Society, Boston, 1982), p. 169; M. C. McCoy, in *Ninth Conference on Probability and Statistics in Atmospheric Sciences* (American Meteorological Society, Boston, 1985), p. 423; *Bull. Am. Meteorol. Soc.* 67, 155 (1986).
 45. D. F. Ransohoff and A. Feinstein, *New Engl. J. Med.* 299, 926 (1978); G. Revesz, H. L. Kundel, M. Bonitabus, *Invest. Radiol.* 18, 194 (1983). Recommendations for handling various bias problems are advanced by C. B. Begg and B. J. McNeil, *Radiology* 167, 565 (1988).
 46. This article was prepared during a sabbatical leave granted under the Science Development Program of BBN Laboratories Incorporated.

The El Niño Cycle: A Natural Oscillator of the Pacific Ocean–Atmosphere System

NICHOLAS E. GRAHAM AND WARREN B. WHITE

Research conducted during the past decade has led to an understanding of many of the mechanisms responsible for the oceanic and atmospheric variability associated with the El Niño–Southern Oscillation (ENSO). However, the reason for one of the fundamental characteristics of this phenomena, its quasi-periodicity, has remained unclear. Recently available evidence from a number of sources

now suggests that the ENSO "cycle" operates as a natural oscillator based on relatively simple couplings between the tropical atmospheric circulation, the dynamics of the warm upper layer of the tropical ocean, and sea surface temperatures in the eastern equatorial Pacific. This concept and recent field evidence supporting the natural coupled oscillator hypothesis are outlined.

ONE OF THE FUNDAMENTAL ASPECTS OF THE EL NIÑO–Southern Oscillation (ENSO) phenomena is its quasi-periodicity that is marked by the repeated appearance of warm or cool water in the equatorial eastern and central Pacific Ocean at intervals of 3 to 5 years. There is now evidence that this quasi-cyclic behavior is due to the operation of a natural coupled oscillator of the ocean-atmosphere system in the tropical Pacific. In the context of this concept, warm and cool water episodes are considered as phases of a self-sustaining cycle; this contrasts with the more traditional view of El Niños as discreet warm events superimposed on a mean background state. This cycle is maintained by

interactions, both immediate and delayed as well as local and remote, between three fields in the tropical Pacific; sea surface temperature (SST), surface wind, and the thickness of the warm upper layer of the ocean. Representative examples of time series from each of these fields are presented in Fig. 1, which shows departures from the long-term monthly means of eastern Pacific SST (1), zonal (east-west) wind in the central equatorial Pacific (2), and sea level at Truk Island in the western tropical Pacific (3) for the period from 1950 through the mid-1980s (4). How these curves

The authors are at the Scripps Institution of Oceanography, La Jolla, CA.

represent key aspects of the natural oscillator concept will be set forth below; for now we wish only to emphasize the quasi-periodic nature of each variable and the apparent close relation among them. Although the approximate periodicity of these and other variables has long been recognized (5, 6), the nature of the interrelations responsible for the cyclic behavior have only recently become clear and are the subject of this article. To set a backdrop for an empirical discussion of this idea, we offer a brief review of the tropical linear ocean dynamics and atmospheric processes needed to understand the workings of the ENSO "cycle."

From a simple linear dynamical point of view, the tropical oceans can be thought of as consisting of a layer of warm light water resting on a much deeper layer of denser cold water. The interface between these layers is called the thermocline; motions within the upper layer are termed baroclinic, meaning they are closely related to the thickness of the warm layer above the thermocline. These baroclinic motions are affected primarily by surface wind stress, which is proportional in magnitude to the square of the wind speed and oriented in the same direction as the surface wind vector. Within two to three degrees of the equator (a region referred to as the equatorial waveguide), the zonal component of the wind stress is of great importance. Here, changes in the zonal wind stress cause changes in the slope of the sea surface and in the thickness of the

upper layer. The balance between the resulting pressure gradients in the upper layer and the Coriolis force causes disturbances, known as baroclinic Kelvin waves, to move rapidly eastward from regions of remote forcing at speeds sufficient to cross the equatorial Pacific in 2 to 3 months (approximately 250 cm s^{-1}). These waves have been studied in detail (7), and there is much empirical evidence to indicate that Kelvin wave activity is associated with the deepening of the thermocline in the eastern equatorial Pacific, which in turn is responsible for the elevated SSTs and high sea levels associated with El Niño (because the water in the upper layer has relatively low density, a deepening of the thermocline results in higher sea levels).

Away from the equator (outside of the equatorial waveguide), the wind-stress curl causes changes in upper layer thickness (ULT) by a process known as "Ekman pumping" (8). This process reflects the fact that cyclonic wind-stress curl forces divergence at the ocean's surface and thereby induces upward vertical motion that decreases the thickness of the upper layer. Conversely, anticyclonic curl results in convergence, downward vertical motion, and increasing upper layer thickness. In off-equatorial regions, the resulting disturbances, known as baroclinic Rossby waves, move westward away from regions of remote forcing at speeds that depend on latitude. These speeds are much slower than those associated with equatorial baroclinic Kelvin waves. Near the equator, the time required for one of these baroclinic Rossby waves to cross the Pacific basin is about 9 months. Further poleward, that time increases sharply; for example, at 12° latitude the basin transit time is about 4 years (9). Until recently, off-equatorial baroclinic Rossby waves have not been generally regarded as playing an important role in the development of El Niño. Rather, the general consensus during the past decade has been that Kelvin waves, which are confined to the equatorial waveguide and forced by changes in zonal wind stress along the equator, both initiate and sustain El Niño events. This latter concept does not provide a satisfactory explanation of the quasi-periodicity of the wind stress changes that force the phase reversals of ENSO (for example, from warm to cool events). In contrast, the coupled-oscillator concept, in which off-equatorial Rossby wave activity is a key element, gives a more robust view of the entire ENSO cycle, of which the classic El Niño is only a part.

Recently available field measurements, numerical model results, earlier theoretical considerations, and other evidence now suggest that the quasi-periodic appearance of warm water in the eastern Pacific (El Niño) is just one aspect of a system that operates as a natural coupled oscillator (the ENSO cycle) of the tropical Pacific Ocean and atmosphere. The interactions that produce these oscillations can be described simply as follows. The response of the surface wind field over the tropical Pacific to SST anomalies in the eastern and central equatorial regions produces two distinct oceanic responses (the case for cool anomalies is presented parenthetically after the case for warm anomalies). First, westerly (easterly) zonal wind stress anomalies within the equatorial waveguide generate the familiar equatorial Kelvin waves that reinforce the current SST anomalies in the eastern and central equatorial Pacific by increasing (decreasing) the thickness of the upper layer in those regions. Second, outside of the waveguide, positive (negative) Ekman pumping produces upwelling (downwelling) baroclinic Rossby waves that propagate westward for times ranging from a few months to 2 years (depending on the latitude and the distance to the western boundary), reflect from the western boundary into the equatorial waveguide as baroclinic Kelvin waves, and eventually reverse the sign of the upper layer thickness (that is, thermocline depth) and SST anomalies in the eastern and central equatorial Pacific. In this way, off-equatorial baroclinic Rossby waves provide the delayed negative feedback necessary for the quasi-periodicity that characterizes the ENSO cycle.

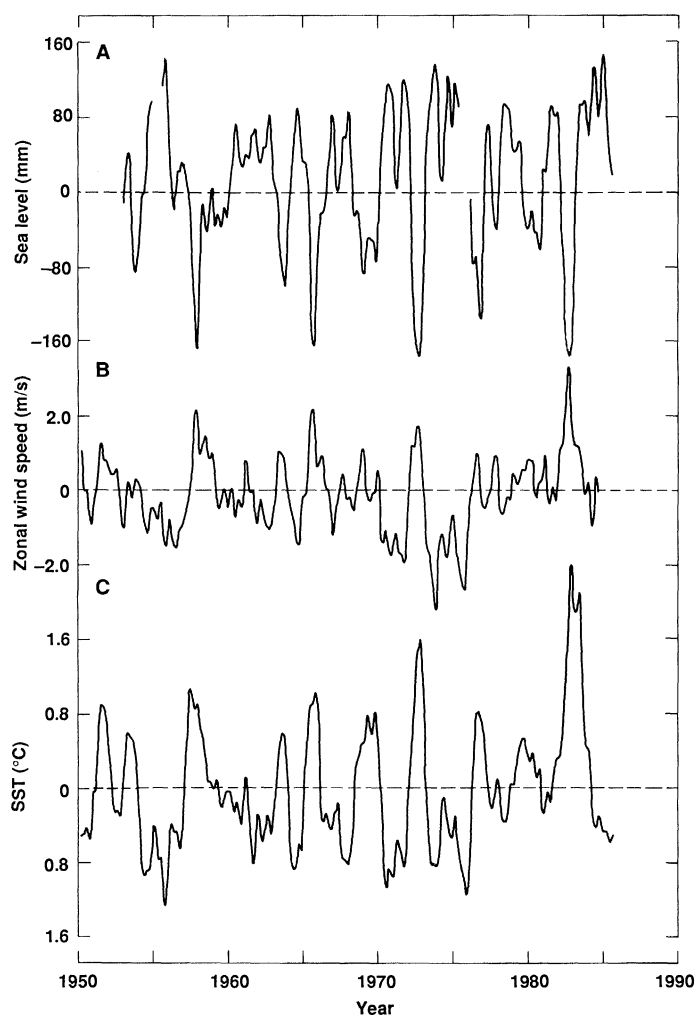
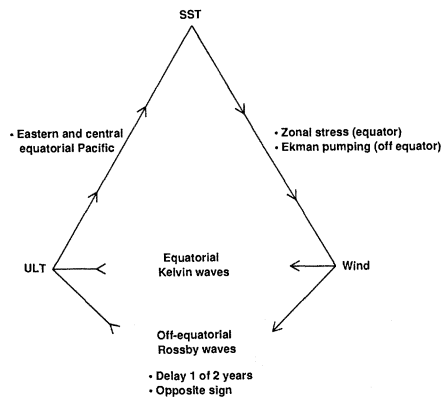


Fig. 1. Smoothed time series of (A) sea level at Truk Island in the western tropical North Pacific (7°N , 152°E , 1953–85); (B) central Pacific zonal wind (3°N to 3°S , 165°W to 155°E , 1950–84); and (C) eastern Pacific SSTs (8°N to 8°S , 86°W to 122°W , 1950–85). Blank portions indicate missing data.

Fig. 2. Coupling diagram for ENSO natural coupled oscillator hypothesis. Arrows denote direction of immediate forcing.



Background

The idea that off-equatorial baroclinic Rossby wave activity could play a role in the development of El Niño was apparently first suggested in work by Godfrey (10), whose numerical model results showed that a free off-equatorial baroclinic Rossby wave would propagate to the western boundary, then equatorward as a coastal baroclinic Kelvin wave, and then eastward along the equator as an equatorial baroclinic Kelvin wave. Although Godfrey did not specifically invoke this process as being important to the idea of an ENSO “cycle,” he was among the first to note that wind-forced equatorial Kelvin waves were a likely cause of the SST and that sea level anomalies in the eastern equatorial Pacific were associated with El Niño.

At about the same time, and referring to Godfrey’s work (10), Wyrтки (6) noted that conditions prior to the onset of El Niño were marked by positive sea level anomalies (that is, a thick upper layer) in the western tropical Pacific and stronger than normal equatorial easterly winds in the central Pacific. Wyrтки reasoned that the sea level anomalies were caused by the strong easterlies and marked the accumulation of warm surface water in the western ocean. Any subsequent weakening of the easterly winds would result in a discharge of this warm water along the equator into the eastern Pacific and the onset of El Niño; equatorial baroclinic Kelvin waves were proposed as a likely mechanism for achieving this redistribution. Although Wyrтки’s hypothesis does not give a mechanism for weakening the equatorial easterlies and does not involve the propagation and reflection of off-equatorial baroclinic Rossby waves, it does contain elements of the coupled oscillator hypothesis and has since been extended (11) to include the idea of a cycle whose period is determined by the time required to recharge the western Pacific with warm water.

McCreary (12) considered the results of (6, 10) and other pioneering tropical ocean modeling efforts (13), together with empirical evidence that opposing changes in the off-equatorial winds (the tradewinds) and the equatorial easterlies associated with ENSO events (14) would produce off-equatorial upper layer thickness anomalies (in response to Ekman pumping) opposite in sign to those responsible for the eastern Pacific SST anomalies. In this summary work, a conceptual coupled ocean-atmosphere model was proposed in which the oceanic component was forced with idealized patches of equatorial and off-equatorial winds that switched on and off depending on the thickness of the upper layer in the eastern equatorial boundary region. Although the behavior and location of the wind field were highly idealized and not fully in agreement with observations, the results of numerical tests of this idea showed that the reflection of off-equatorial Rossby waves from the western boundary allowed this coupled ocean-atmosphere system to oscillate quasi-periodically in a way that resembled the ENSO cycle. The

concept was not generally accepted at the time of its publication because of the artificial wind system used and because the relatively long transit times of the baroclinic Rossby waves made their survival seem unlikely. Rather, the interpretation of observations available at the time supported the view that El Niños were broad-band signals in a chaotic system (15, 16). In this study, consideration of recently available field data and historical observations, and reinterpretation of earlier results, show El Niño to be one phase of a low-frequency oscillation of the tropical ocean-atmosphere system, that is the ENSO cycle.

Recently, Schopf and Suarez (17) have explicitly identified the delayed negative feedback provided by off-equatorial baroclinic Rossby waves as the cause of quasi-periodic ENSO-like oscillations in their coupled tropical ocean-atmosphere model. This model uses a global two-layer atmosphere driven by parameterized heat exchange with a tropical ocean and a specified equator-to-pole temperature gradient. The rectangular model ocean, which is 160° wide longitudinally and extends from 20°N to 20°S, has three layers in which the temperature, thickness, and velocity are simulated. The layers are coupled to each other through vertical motion and diffusion. The upper layer is coupled to the atmosphere through a simple parameterization of combined sensible and latent heat flux and surface wind stress (taken to be proportional to the wind at 750 mbar, about 3000 m above the surface).

In a 35-year integration, this model showed well-organized anomaly patterns in the atmosphere and ocean that exhibited quasi-periodic oscillations with periods of 4 to 6 years that are qualitatively similar to those observed in association with the ENSO cycle. Analysis of the model results showed that the oscillations were due to positive feedback between the zonal equatorial winds and eastern equatorial Pacific SSTs at relatively short time scales, and, at longer time scales, the delayed negative feedback provided by the reflection of off-equatorial baroclinic Rossby waves from the western boundary and their subsequent manifestation in eastern equatorial Pacific SSTs.

Further evidence that ENSO-like oscillations in coupled tropical ocean-atmosphere models are due to the correct simulation of real physical processes comes from the successful forecast model results

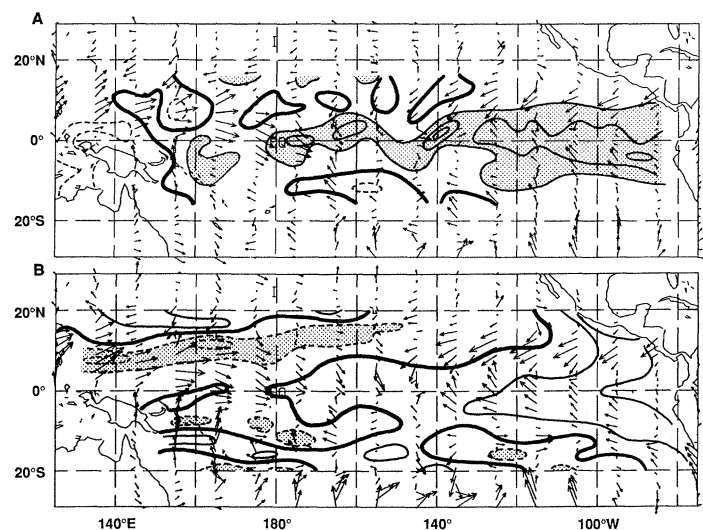
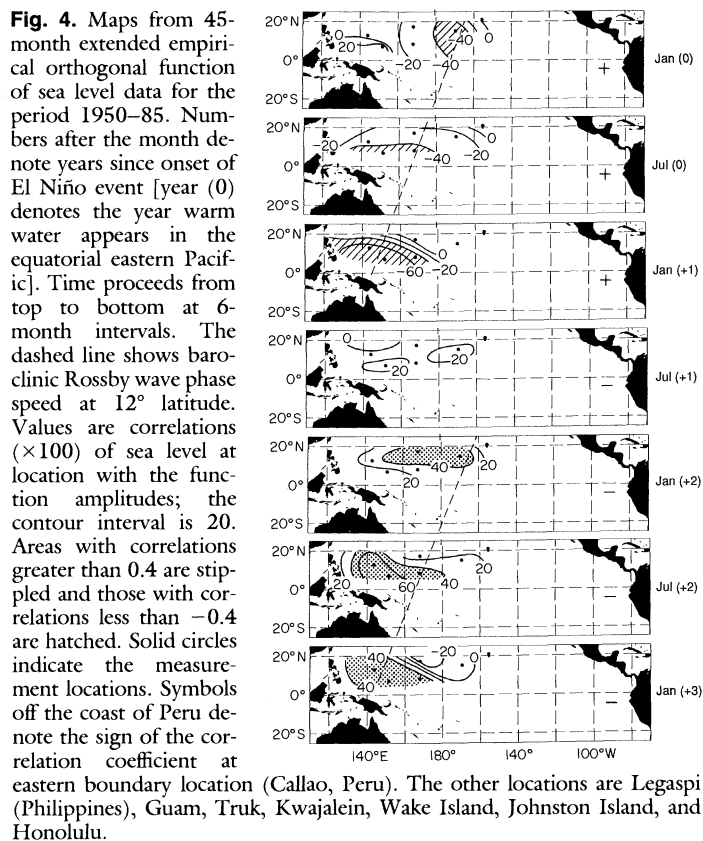


Fig. 3. Canonical correlation patterns for: (A) SST (16°N to 16°S) and surface wind stress (30°N to 30°S) for the period 1962–84; and (B) the FSU model results for ULT (20°N to 20°S) and surface wind stress (30°N to 30°S) for the period 1962–84. Negative contours are dashed, the zero contour is the heavy line. Values are relative weights; contours are evenly spaced. Stippling indicates a major positive SST anomaly in A and a major negative ULT anomaly in B.

reported by Cane and Zebiak (18) in several papers. This model, although somewhat simpler than the Schopf-Suarez formulation, also produces ENSO-like quasi-periodic behavior and was used to successfully forecast the 1986–87 El Niño 9 months in advance (19). Trials that used data from the 1960s to the present have shown that this model has the potential to produce generally reliable El Niño forecasts at lead times up to a year or more.

Two major differences between the Cane-Zebiak model and the Schopf-Suarez model probably contribute to the former's forecasting success. First, the model allows feedback between latent heat release in areas of organized convection and the wind field, which supplies much of the water vapor that fuels the convection through mass convergence. This feedback contrasts with the Schopf-Suarez model, in which there are no moist processes and atmospheric heating is due to changes in surface temperature only. A second major difference is that many of the parameters in the Cane-Zebiak model (for example, SST, ocean currents, surface winds, and ULT) are expressed as departures from a climatology prescribed in terms of monthly averages. These averages are determined either from the observed climatology (SST and surface winds) or from the climatology of the ocean model forced with observed wind stress (currents and ULT). Although this scheme makes the model less realistic than that of Schopf and Suarez, it does remove the constraint that the model successfully simulate both climatology and anomalies, thereby facilitating better simulation of nonlinear interactions between the mean and anomaly fields. Although the issue of western boundary reflection in causing the oscillatory behavior in their model has not been specifically addressed by Cane and Zebiak, recent experiments by Battisti with a similar model (20) show that the oscillations cease if the western boundary is made nonreflective. This finding indicates that the delayed negative feedback–reflected Rossby wave mechanism sustains the model ENSO cycle, as suggested by Graham *et al.* (21) and Schopf and Suarez (17).



Evidence for the delayed negative feedback role of off-equatorial baroclinic Rossby waves also comes from unsuccessful attempts to model El Niño events without consideration of the importance of the preceding cool water phase of the ENSO cycle. In a modeling study described by Cane (22), an ocean model was driven with winds composited from several El Niño events by Rasmusson and Carpenter (23). These composites begin just before the onset of an El Niño event and thus do not cover the preceding cool SST phase of the ENSO cycle, during which time the delayed feedback hypothesis calls for downwelling baroclinic Rossby waves to be generated in the off-equatorial western and central tropical Pacific. The results showed that the modeled thermocline fluctuations that mark the onset of the El Niño were much smaller than those that would be expected from sea level observations. Later, during the mature stage of the modeled composite event, the agreement between the modeled ULT and observed sea level data was much better. The inability of a model driven in this way to simulate the onset of El Niño is as expected from the hypothesis under consideration, since the eastern Pacific ULT anomalies observed at the onset of El Niño have their genesis during the previous cool water phase, a period not included in the simulation. Later in the warm event of the model, rising eastern Pacific SSTs (reflecting the deepening thermocline there) cause the usual equatorial easterlies to collapse, resulting (through wind-forced Kelvin waves) in the major thermocline depth and SST anomalies that mark the height of the warm phase of the ENSO cycle. Note that when similar models are driven with longer periods of wind data that do include the previous cool water phase (24, 25), the hindcast El Niño onsets are much better. This fact, taken with the less successful results from the truncated simulation (22), lends further support to the importance of the delayed negative feedback mechanism in forcing ENSO phase reversals.

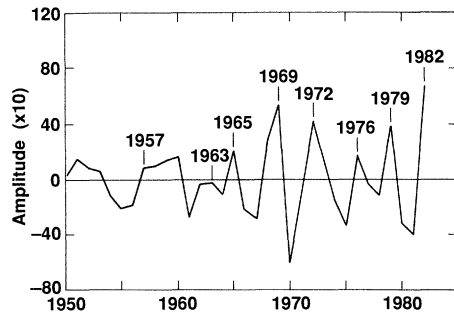
Similar arguments can be used to explain the behavior of statistical models (21) designed to forecast eastern equatorial Pacific SSTs on the basis of near-equatorial winds during the previous 6 to 11 months. These models also show good skill during the mature stage of El Niño events, but appear to be unable to forecast the rapid rises in SST that often occur at the onset of the warm phase. As outlined above, such behavior is as expected from the delayed negative feedback-coupled oscillator concept, because the predictor data used by the model do not extend far enough back in time nor do they reach far enough off the equator to forecast the onset of El Niño events. In agreement with this interpretation is the successful forecast of the onset of the 1986–87 El Niño by a statistical model based on measurements of Rossby wave activity from the off-equatorial western Pacific during the previous 1 to 2 years (26).

Thus evidence from theoretical and statistical models support the idea that the quasi-periodicity of the ENSO cycle is the manifestation of a natural coupled oscillator in the ocean-atmosphere system of the tropical Pacific. However, we know of few published studies that provide further support for this concept on the basis of comparisons of field observations and model results. In the section below, we outline the key dynamical links that allow the coupled oscillator to operate and present new field observations, statistical analyses, and model results that support their existence.

The Conceptual Model: Outline and Evidence

The natural coupled oscillator concept of the ENSO cycle can be described on the basis of the interactions between three fields in the tropical Pacific: SST, surface wind stress, and ULT on and off the equator. These interactions are summarized by the coupling diagram shown in Fig. 2. If we take SST as a starting point (27), the

Fig. 5. Amplitudes of sea level extended empirical orthogonal function shown in Fig. 4. Major El Niño events are indicated; the vertical scale is in relative units.



ENSO cycle requires that eastern and central Pacific equatorial SST anomalies cause changes in the tropical wind field. This event is followed in the diagram by the requirement that changes in the tropical wind stress field result in changes in the ULT field. The two responses are shown for this relation; one represents the equatorial baroclinic Kelvin wave response (short delay and positive feedback) that results from changes in zonal wind stress within the equatorial waveguide, and the other represents the off-equatorial baroclinic Rossby wave response (long delay and negative feedback) resulting from changes in the off-equatorial Ekman pumping. The Rossby wave response provides this negative feedback at the time scales of 1 to 2 years required for westward propagation and wave reflection from the western boundary onto the equator and into the eastern equatorial ocean. The ENSO cycle is completed by the requirement that changes in ULT in the eastern and central equatorial ocean force changes in SST there, because the mean zonal wind stress in this region (even during the warm phase of the ENSO cycle) is easterly, resulting in equatorial upwelling. The degree to which this upwelling reduces SSTs is determined by the thickness of the upper layer; when the upper layer is relatively thick, water circulated upward by the upwelling is warmer than it would be if the upper layer were relatively thin. In the discussion that follows, we outline evidence for each of these relations.

The SST forcing–wind stress relation depicted in Fig. 2 is well accepted. Evidence that equatorial zonal wind anomalies are associated with SST anomalies is available from statistical analyses of observations (14, 23, 28, 29). Furthermore, although this is a positive feedback relation, which makes it difficult to separate cause from effect by using observations alone, numerical and analytic atmospheric models provide clear evidence that SST anomalies are responsible for the wind field anomalies observed in association with ENSO (30). The response of the atmospheric circulation to anomalous SSTs is not only due to changes in surface temperature gradients (that is, a dry atmosphere response), but also to anomalous atmospheric latent heating that reflects changes in the distribution of large-scale, organized convective activity (a moist atmosphere response). A significant amount of the anomalous energy released to the atmosphere during the warm phase of the ENSO cycle (El Niño) may come from this latter process, which is mediated in turn by the convergence of water vapor rather than local evaporation (18, 31). Because organized convection occurs only during major El Niños in some areas and thus has a skewed (non-Gaussian) distribution, and since there is a rather sharp threshold in SST below which large-scale convection does not occur (32), the atmospheric circulation anomalies associated with the warm water phase of the ENSO cycle are probably not simply reversals of those that occur during the cool water phase. Thus the cycle is not perfectly symmetric and some variables do have skewed distributions, as is apparent from the Truk Island sea level and eastern-Pacific SST time series in Fig. 1.

New statistical analyses of observations provide further support

for the close relation between the ENSO SST and surface wind stress fields. For example, Fig. 3A shows the SST and wind field patterns typically found in July at the beginning of the warm phase of the ENSO cycle. These SST observations come from commonly used sources (1) and the wind stress data were compiled at Florida State University (FSU) (33). The analysis described here covers the period 1962–84. The statistical technique used to generate these patterns is known as canonical correlation analysis, a powerful method of investigating the relation between two fields (28, 34). In this case, the panel shown is one of a sequence of maps covering 21 months of evolution of the two fields extending from the end of the cool water phase of the ENSO cycle through the warm phase and into the following cool phase. The squared correlation (the canonical correlation) between the time series of these modes of evolution in each field is 0.89, demonstrating that the relation between the fields is very close, that is, when the SST field looks like the pattern shown, the wind field is very near that depicted in the Fig. 3A. The important features to note in Fig. 3A are the warm SST anomalies in the eastern and central equatorial Pacific, westerly wind stress anomalies just north of the equator in the western Pacific (35), and generally easterly wind stress anomalies farther away from the equator. This pattern results in generally positive (upwelling) Ekman pumping (and an anomalously thin upper layer) in the off-equatorial western and central ocean on both sides of the equator.

The Kelvin wave segment of the wind stress–ULT link in the coupling diagram (Fig. 2) is also widely accepted. Equatorially trapped baroclinic Kelvin waves have been studied in detail in many numerical ocean modeling studies [for example, (22, 24, 25, 36)], the results of which compare well with sea level observations. In addition, field observations from instrumented moorings along the equator (7) as well as satellite altimetric data (37) have verified their presence. In contrast, the delayed negative feedback mechanism associated with the off-equatorial baroclinic Rossby wave segment of the second leg of the coupling diagram is not widely accepted, although the presence of positive sea level anomalies in the western off-equatorial Pacific prior to the onset of El Niño events and of negative sea level anomalies during the warm phase of the ENSO cycle has been described by several authors (6, 11, 14, 38). Other observational and numerical modeling studies have associated these features with off-equatorial baroclinic Rossby wave activity (9, 24, 26, 39).

In view of the agreement between the modeled and observed sea level data (24, 39, 40), we applied canonical correlation analysis to calculate the wind stress anomaly patterns associated with typical model ULT anomaly fields, as is shown in Fig. 3B with the same wind data described for Fig. 3A and monthly ULT data from the FSU linear ocean model described in (24). This model has been shown to closely reproduce observed changes in the thickness of the upper layer of the tropical Pacific (24–26, 39–41) in many studies, and comparisons between the relatively simple linear FSU model and more elaborate nonlinear ocean models (17) suggest only minor differences in the major low-frequency signals.

As with the application of this statistical technique to the monthly SST and wind stress anomalies patterns described above, the period used in this calculation was 1962–84, and here again the canonical correlation is high (0.85), indicating close agreement between the fields. Like Fig. 3A, the panel shown in Fig. 3B shows conditions in July at the beginning of the warm water phase of the ENSO cycle. The westerly wind stress anomalies along the equator produced positive ULT anomalies in the eastern equatorial Pacific, in general agreement with the SST anomalies found there in Fig. 3A. Off the equator in the western and central tropical North Pacific, anomalous Ekman pumping has resulted in a region of negative ULT anomalies (that is, a shallow thermocline). This effect is not reflected in the

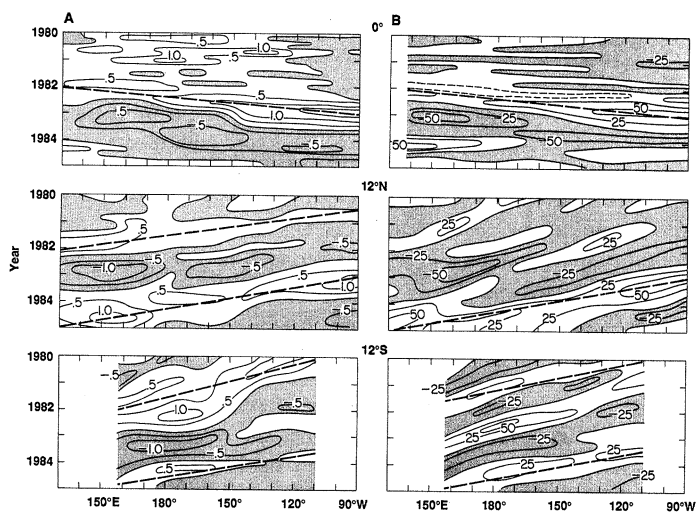


Fig. 6. Time-longitude sections of (A) anomalous T_{av} and (B) FSU model and ULT for 1980–85; equator (top), 12°N (middle), and 12°S (bottom). Shaded areas denote negative anomalies. Dashed lines emphasize major propagating positive anomalies and indicate phase speeds of 10 to 20 cm s^{-1} at 12° latitude and 50 to 100 cm s^{-1} on the equator. Contour interval is 0.5°C for T_{av} and 25 m for ULT.

SST pattern in Fig. 3A, because the mean depth of the thermocline in this region (and in the western tropical Pacific in general) is sufficiently deep that large ULT anomalies do not produce large SST anomalies. Similar panels from later in the sequence show the amplification, westward propagation, and reflection of this anomalous ULT feature and the similar but weaker feature visible in the western and central tropical South Pacific. The major point to be noted in comparing Fig. 3, A and B, is the similarity between the wind fields in the two figures. This similarity suggests that the anomalous wind field response to SST anomalies is the same one responsible for generating and amplifying the modeled upwelling off-equatorial Rossby waves during warm phase (and downwelling waves during the cool phase) of the ENSO cycle.

The required points of westward propagation and reflection, although supported by the statistical results mentioned above and by the coupled modeling results described earlier (14), have been reported only from field measurements of vertically averaged temperature (T_{av}) through the upper 400 meters of the ocean (9, 26, 39), a parameter that is closely connected with thermocline depth. These observations come from expendable bathythermograph (XBT) measurements made by research and volunteer merchant and fishing vessels across the tropical Pacific as part of the Tropical Ocean–Global Atmosphere (TOGA) program. Analyses of these data (8, 26, 39) have shown that the westward propagation of baroclinic Rossby waves can be tracked across the off-equatorial tropical Pacific and into the equatorial waveguide. The actual reflection process, in which the wave energy is conducted along the western boundary into the waveguide, has not been observed, but is inferred from the continuity of the on- and off-equatorial T_{av} measurements. The lack of actual observations of thermocline anomalies propagating along the boundary, and the difficulty in modeling or theoretically determining details of the expected behavior of long baroclinic Rossby wave activity impinging on a ragged boundary such as that of the maritime subcontinent, are controversial problems that require further efforts to resolve.

Although the reflection process remains poorly understood, analyses (26, 39) have shown that the presence of a downwelling wave (an anomalously thick upper layer) at the western boundary in boreal fall and winter signals the onset of the warm phase of the

ENSO cycle (El Niño) the following year, as would be expected from the reflected baroclinic Rossby wave mechanism. A major finding of the work with the XBT data has been that comparisons with ULT data taken from the wind-forced FSU ocean model show good agreement, both with respect to the dominant patterns of interannual variability (41), and on the points of apparent reflection and westward propagation (26). This relatively good agreement between observed T_{av} and model ULT data is important, because the T_{av} data are available only since 1979 and suffer from irregular spatial coverage, whereas the FSU model data are gridded and available since 1962. The agreement between the model ULT and observed T_{av} data from 1979–84 supports the use of the model data to study the behavior of off-equatorial baroclinic Rossby waves over the last 25 years for which model data are available.

Because the reflection of westward propagating Rossby waves at the maritime western boundary of the Pacific is probably the least well-accepted element of the natural coupled oscillator concept (because of the irregular, nonsolid boundary), we also present new statistical analyses of tide-gauge sea level observations (3) and ocean model ULT data that support this mechanism. First, we have analyzed sea level observations from tide gauges at six locations in the tropical western North Pacific and one station on the eastern boundary over the period 1950–85 with a technique known as extended empirical orthogonal function analysis. Much like ordinary empirical orthogonal functions, which objectively portray typical patterns of static variability in a field, extended empirical orthogonal functions allow the depiction of the dominant patterns (or modes) over time. The technique has proven of great value in portraying the evolution of various fields in association with the ENSO cycle (28, 42). Figure 4 shows a sequence of maps from such a mode covering the development of sea level anomaly patterns for a 45-month period beginning in January. The mode shown is the second most dominant, accounting for 12% of the total variance (43).

The pattern across the western North Pacific in Fig. 4 is one of slow westward propagation, with the presence of an anomaly of one sign at the western boundary in January preceding the presence of a liked-signed anomaly along the eastern boundary in the following July, that is, a change in the phase of the ENSO cycle. For reference purposes, the free baroclinic Rossby wave speed for 12° latitude from the FSU ocean model (44) is shown in Fig. 4 as well and can be seen to be in agreement with the trend of the motion. That this pattern is the one associated with the ENSO cycle is demonstrated in Fig. 5, which shows the amplitudes of the empirical orthogonal function shown in Fig. 4. The amplitudes simply measure how much the evolution of the observed sea level data over a given period resembles the pattern shown in Fig. 4. These amplitudes typically show low values prior to, and peaks during, the major El Niño events over the past 36 years, clearly supporting the contention that upwelling off-equatorial Rossby waves generated during the warm eastern Pacific SST phase (and downwelling waves during the cool phase) of the ENSO cycle later force a change in the sign of the eastern equatorial SST anomalies; that is, a reversal of phase of the ENSO cycle.

As noted above, the T_{av} data reported in (8, 26, 39) appear to agree with numerical results from the wind-forced FSU ocean model. An example of this agreement is given in Fig. 6 which shows time-longitude sections of observed T_{av} and model ULT data at 12°N, 12°S, and along the equator during the 6-year period 1980–85. Qualitatively, the agreement between the observations and model data is good, not only with respect to individual features, but also in showing westward propagation along 12°N and 12°S and the eastward propagation along the equator. Note that the incidence of the Rossby wave activity at the western boundary in late 1981 and

early 1982 at those latitudes was followed by reflections along the equator to the eastern boundary (the bimonthly resolution of the data shown here is too coarse to consistently resolve baroclinic Kelvin wave propagation). The slow propagation (50 to 100 cm s^{-1}) along the equator of the major thermocline anomalies has been observed in other fields (23, 28, 45) in association with the evolution of El Niño events, and is also apparent in the coupled model results of Schopf and Suarez (17). This behavior is thought to represent a nonlinear coupled ocean-atmospheric disturbance involving large-scale convection, SST, and the wind field in the near-equatorial tropics, and is closely associated with the sustained atmospheric anomalies that mark the warm phase of the ENSO cycle.

Another interesting feature in Fig. 6 is the apparent reflection from the eastern boundary of the positive anomalies associated with the 1982–83 ENSO event as baroclinic Rossby waves along 12°N and 12°S and their subsequent trans-Pacific propagation. Indeed, more recent analyses suggest that these waves may be connected with the phase change of the ENSO cycle marked by the onset of the 1986–87 El Niño event. Whether eastern boundary reflection is important to maintaining the coupled oscillations is unclear; it is not invoked in this study. It is conceivable, however, that this mechanism of reflection from the eastern boundary could provide correctly signed features in the western and central off-equatorial Pacific that later undergo further wind-forced amplification at the extremes of the ENSO cycle.

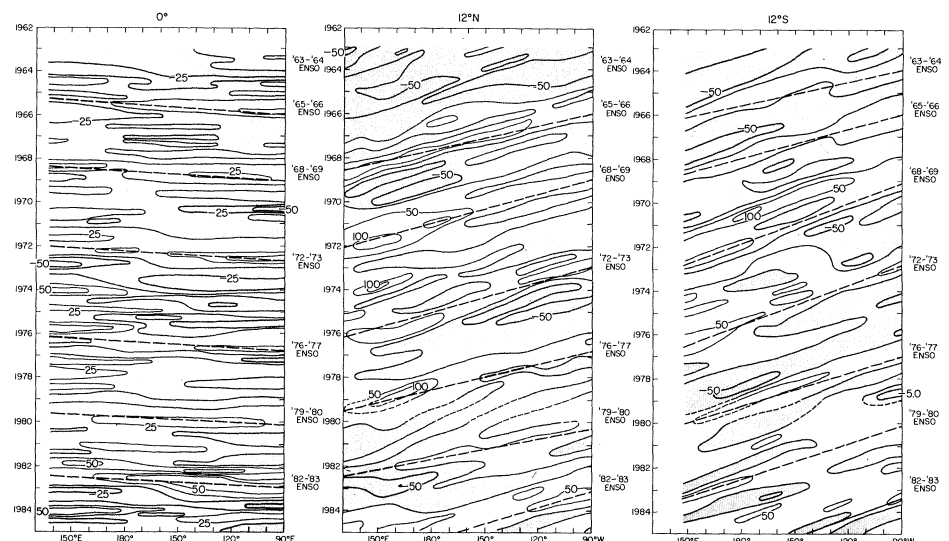
The agreement between the T_{av} data and the FSU-model ULT data [as well as agreement between model ULT and tide-gauge sea level data (25, 39, 40)] supports the use of model data to study the evolution of ULT anomalies. To do this, we show the time-longitude sections of model ULT anomalies for the equator, 12°N, and 12°S for the 21-year period 1964–84 in Fig. 7. Although clouded somewhat by a long-term trend for the model to raise ULT over much of the tropical Pacific, the patterns are much like those seen in Fig. 5, with clear indications of westward propagation and apparent reflection from the western boundary of off-equatorial anomalies preceding major warm (and cool) phases of the ENSO cycle. Reflections of equatorial baroclinic Kelvin waves from the eastern boundary as baroclinic Rossby waves are also seen, with subsequent amplification in the central and western Pacific. As noted above, the significance of this last element to the coupled oscillator concept is unclear and is not a required link in the scenario described here. Also note that, as outlined here, the coupled oscillator concept does not assume that the off-equatorial baroclinic Rossby wave activity responsible for phase reversals in the ENSO

cycle always occurs at a particular latitude or within a particular hemisphere. Nor do we propose that nonlinear interactions or stochastic forcing arising internally within the coupled system in the tropical Pacific, or elsewhere in the tropics or extra-tropics, does not play important roles in determining the characteristics of the quasi-cyclic behavior. Rather, the thrust of the coupled oscillator concept is that the coupled system will tend to oscillate, perhaps irregularly, once disturbed, and that these oscillations are modulated primarily by the delayed negative-feedback mechanism.

To complete this discussion of evidence for the off-equatorial baroclinic Rossby wave link in the ocean-atmosphere coupled oscillator concept, we present an extended empirical orthogonal function representing the variability of the gridded FSU model ULT data covering the 23-year period 1962 through 1984 in Fig. 8. In this case the function covers a 21-month period beginning in January, with 3-month intervals between maps. The pattern shown is the second mode (12% of the total interannual variance); the first mode centered on the tendency of the model to gradually raise ULTs over much of the tropical Pacific, as noted in the discussion above. The panels show the onset of a warm event in April [marked Apr (0)], with positive ULT anomalies (that is, a deep thermocline) becoming established in the eastern equatorial Pacific during the following July, October, and January. At the same time, the amplification and slow westward progression of upwelling baroclinic Rossby waves (negative ULT anomalies) in the central and western ocean can be seen, as can the poleward spread of the thermocline anomalies along the eastern boundary (through baroclinic coastal Kelvin waves) and their reflection into the interior (as baroclinic Rossby waves). In the sixth panel [marked Apr (+1)], reflection of the upwelling Rossby waves off the western boundary has occurred, and the passage of baroclinic Kelvin waves is marked by the eastward spread of negative ULT anomalies along the equator, as shown by the position of the zero contour. In the subsequent two months, the panels show the continued development of negative ULT anomalies in the eastern and central equatorial ocean and the westward propagation of Rossby waves, whose curved shape reflects the latitude dependence of their phase speeds. Another mode from this analysis shows further development of the eastern Pacific thermocline depth anomalies and completes the cycle.

The final link of the ocean-atmosphere coupling diagram (Fig. 2) shows that thermocline depth has an important effect on SSTs in the central and eastern Pacific. Although this relation has been well established (14, 24), we present further evidence in Fig. 9A, which shows model ULT anomalies and SST anomalies in the eastern

Fig. 7. Time-latitude sections of FSU model ULT 1963–85 for equator, 12°N, and 12°S; major El Niños are indicated. Negative anomalies are shaded; the contour interval is 25 m. Dashed lines emphasize major propagating positive anomalies and indicate phase speeds of 10 to 20 cm s^{-1} at 12° latitude and 50 to 100 cm s^{-1} on the equator.



Pacific (8°N to 8°S and 86°W to 122°W) for the period 1962–84. The agreement between the data sets is close (the correlation is 0.71). The agreement in the central Pacific is not as good (suggesting the importance of other processes in determining SST), although by using monthly data for 1956–86, the correlation between Christmas Island sea level (2°N, 157°W) and SSTs in the region bounded by 4°N and 4°S, and 154°W and 162°W, is 0.59, with sea level leading by one to two months.

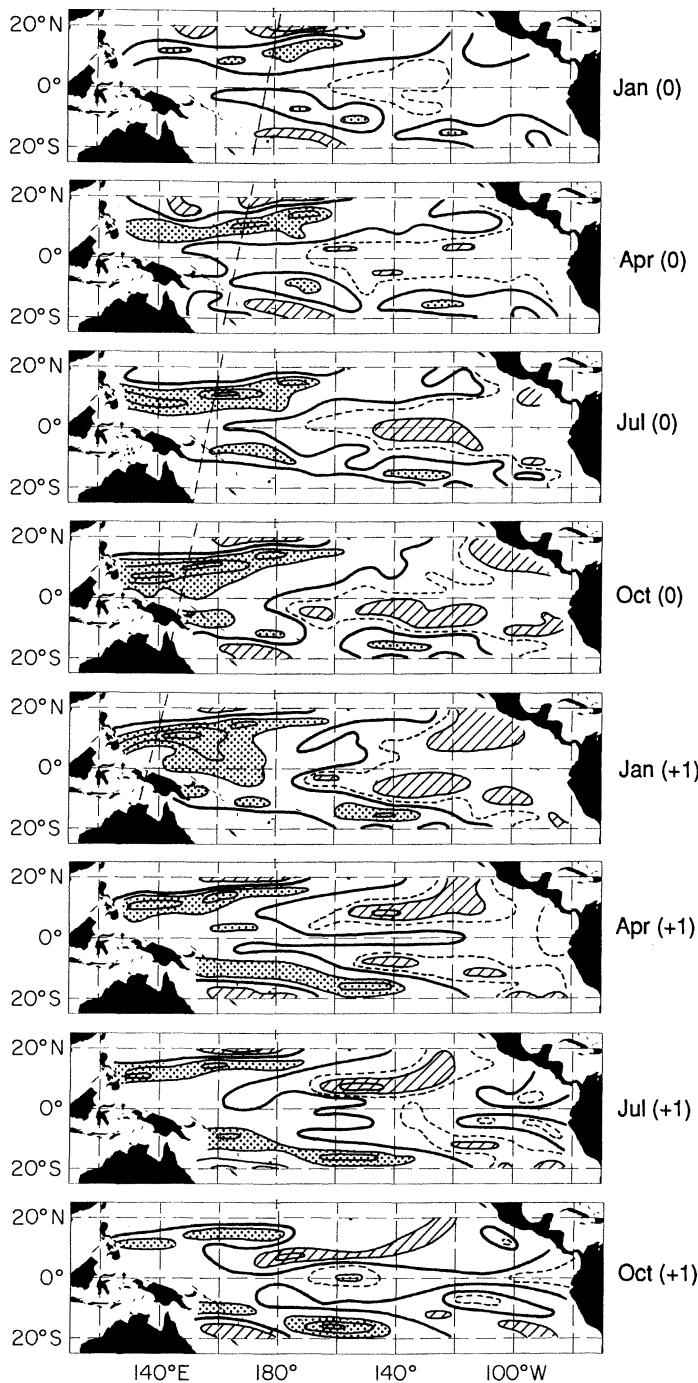


Fig. 8. Maps from 21-month extended empirical orthogonal function of ULT data from the FSU ocean model for the period 1962–84. Numbers after the month indicate the years since onset of El Niño event. Time proceeds from top to bottom. Values are relative; solid contours are evenly spaced at 10 units, and the zero contour is the heavy line. Regions with weights more than 10 units are hatched, and those less than -10 are stippled. Where shown, dashed contours are 5 units.

Although the association between ULT and SST as we have described it is a strong linear one and has been shown in model results (17, 20) to be responsible for much of the SST signal in the eastern ocean, there are other nonlinear processes that are important contributors to SST variability in the equatorial central and eastern Pacific. These processes have major effects on the details of the timing and distribution of ENSO-related phenomena. Most important among these are the advection of anomalous SSTs by the mean meridional (north-south) currents and the interactions between mean and anomalous ULT and oceanic vertical motion. Battisti's results (20) suggest that the former process is particularly important in sustaining El Niño events, and the latter plays an important role in determining the timing of the amplification of the warm phase of the ENSO cycle in relation to the seasonal cycle.

Concluding Remarks

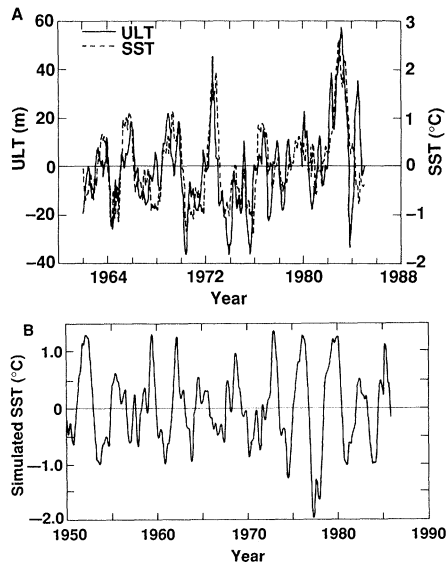
We have presented evidence that the quasi-periodic nature of ENSO phenomena reflects a natural coupled oscillation involving the dynamics of the tropical Pacific ocean and the overlying atmosphere. Classic El Niño events and the related oceanic and atmospheric anomalies represent one phase of this ENSO cycle. This cycle is maintained by a three-part system involving the forcing of the tropical wind stress field by equatorial SST anomalies, the generation of ULT anomalies (baroclinic Kelvin and Rossby waves) by those wind field changes and their subsequent propagation and reflection, and finally the effects on SST by the ULT anomalies in the eastern and central equatorial ocean. Much of this presentation has dealt with two key, but previously poorly documented, elements required to sustain the cycle: the generation of off-equatorial Rossby waves by anomalous Ekman pumping and their subsequent reflection from the maritime western boundary. This mechanism provides the delayed negative feedback necessary to reverse the phase of the system and is responsible for the observed 3- to 5-year time scale of the ENSO cycle. This does not necessarily imply that the oscillations should be perfectly periodic; both the influences of nonlinear effects and stochastic forcing (internal or external) could easily account for the observed quasi-periodicity.

To demonstrate this idea, consider a simple linear simulator of the coupling relations depicted in Fig. 2. Such a conceptual model has four components expressed as anomalies from their mean states: zonal wind stress in the central equatorial Pacific (*ZWS*), sea surface temperature and ULT in the eastern equatorial Pacific (*ESST* and *EULT*), and ULT in the central off-equatorial Pacific (*CULT*). These variables are assumed to be coupled as shown below:

$$\begin{aligned} EULT_t &= a ZWS_t + \rho CULT_{t-\delta} \\ ESST_t &= b EULT_t \\ CULT_t &= -c ZWS_t \\ ZWS_{t+1} &= \alpha(ab)^{-1} ESST_t + \epsilon_t \end{aligned}$$

The subscripts denote a time index, and the constants *a*, *b*, and *c* are positive values representing the observed relations between anomalies in zonal wind stress, eastern Pacific SST, and ULT in the eastern equatorial ocean and in the off-equatorial western and central Pacific (46). These values were selected simply by inspection of time series and scatter plots of these variables. The parameter *p* represents a reflection coefficient and controls the fraction of the off-equatorial ULT anomaly on the western boundary at time *t* (and generated at lag *δ* months prior in the off-equatorial ocean) that is transmitted to the equatorial waveguide and into the eastern ocean as delayed negative feedback; here *p* is assigned a value of 0.1. The time lag parameter (*δ*) was assigned a value of 18 months, repre-

Fig. 9. (A) Time series of FSU model ULT (solid, left axis) and SST (dashed, right axis) anomalies for 1962–84. Anomalies were averaged over the region bounded by 8°N to 8°S latitude and 86°W to 122°W longitude. (B) Time series of eastern equatorial Pacific SST from a simple linear simulator of the coupled oscillator–delayed negative feedback model for the ENSO cycle. The time scale is in years; the starting point in 1950 was arbitrarily chosen to match the plots in Fig. 1.



sentative of the time required for the propagation of major off-equatorial ULT anomalies from the central ocean to the western boundary and into the eastern equatorial Pacific (47). The variable ϵ represents random atmospheric forcing (“weather”). The presence of such high-frequency variability in the tropical atmosphere is well documented (48). For the sake of simplicity, we used uniformly distributed random values with a range of $\pm 1.5 \text{ ms}^{-1}$. Finally, the parameter α , which represents damping within the system, has been given a value of 0.8.

This conceptual model was started from a state of rest (all values 0) and was run forward for a period of 50 years with a time step of 1 month. Quasi-periodic oscillations began within a few years and by the fifth year reached statistical equilibrium. As an example of the model’s behavior, Fig. 9B shows eastern equatorial Pacific SSTs for years 5 through 41 [filtered as in (4)]. The model produced irregular oscillations resembling those seen in observed eastern Pacific SSTs (Fig. 1), with “El Niños” occurring at intervals of about 3 to 5 years. This conceptual model, although very simple, demonstrates that a coupled oscillator–delayed negative feedback mechanism like that described in Fig. 2 can produce quasi-periodic oscillations qualitatively like those observed.

Note that because this simple system is a damped oscillator, external forcing is required to drive the system; delayed negative feedback provides the mechanism that allows for oscillatory behavior. Further, because the relations are expressly linear, the system is not intrinsically chaotic, as was suggested by Vallis (16). When the oscillations are small (that is, the system is near its mean state), the system has little predictability and is primarily influenced by random forcing. When the oscillations are large, the system is more predictable and is primarily influenced by the delayed feedback mechanism. Schopf and Suarez (17) found that oscillations in their model appear to arise from similar mechanisms; that is, they are not manifestations of classic chaotic behavior resulting from nonlinear dynamics, but rather are due to the integration of high-frequency atmospheric (and oceanic) variability by the coupled system. Battisti (20) reached a similar conclusion and produced realistic aperiodicity in his coupled model by introducing a modest amount of stochastic forcing to the zonal wind. Also, Vallis (49) showed that the behavior of a nonchaotic but stochastically forced model could resemble that of a chaotic model.

An understanding of the dynamical nature of the ENSO cycle offers the potential for much improved forecasts of the future state of the ENSO system in general and El Niño in particular. This predictability is related to both the delayed response of eastern

Pacific SSTs to off-equatorial influences and to the approximate linearity of the integrated dynamic response of the oceanic component of the coupled system to relatively high-frequency input from the atmosphere. These factors allow subtle trends in the atmospheric system to be integrated by the oceanic system and expressed later as major low-frequency signals. With improved coupled tropical ocean-atmosphere models, it seems likely that skillful forecasts of parameters such as SST, ULT, and wind stress may sometimes be possible at lead times of many seasons. However, it is inevitable that the ENSO cycle, like mid-latitude weather, will lose predictability to the chaotic forcing that sustains it, although (owing to the long-lasting oceanic signal) at time scales of several years instead of several days. To the degree that the tropical ocean and atmosphere bear on the extra-tropical circulation, such improvements in predictive skill may assist in long-range forecasts of the mid-latitude climate.

REFERENCES AND NOTES

1. We used a combination of SST data from the Comprehensive Ocean-Atmosphere Data Set and from the Climate Analysis Center of the U.S. National Weather Service. These are referenced in R. J. Slutz *et al.*, *The Comprehensive Ocean-Atmosphere Data Set, Release 1* (Climate Research Program, Environmental Research Laboratory/National Oceanic and Atmospheric Administration, Boulder, CO, 1985) and R. W. Reynolds, *Natl. Oceanic Atmos. Adm. (U.S.) Tech. Rep. NWS 31* (National Meteorological Center, Silver Spring, MD, 1982).
2. These wind data come from a composite data set constructed from ship observations at the Scripps Institution from an existing Pacific data set [K. Wyrski and G. Meyers, *J. Appl. Meteorol.* **15**, 698 (1976)] and other data from the Pacific and Indian Oceans [T. P. Barnett, *Mon. Weather Rev.* **111**, 756 (1983)].
3. Sea level data kindly provided by K. Wyrski.
4. Each time series in Fig. 1 was smoothed with a cosine taper filter, with a 3-month half-width and a 0.1 power point at 5 months.
5. J. Bjerknes, *Mon. Weather Rev.* **97**, 163 (1969); W. Quinn, *J. Appl. Meteorol.* **13**, 825 (1974). The first gives further historical references.
6. K. Wyrski, *J. Phys. Oceanogr.* **5**, 572 (1975).
7. C. C. Eriksen, *ibid.* **13**, 1622 (1983); *ibid.* **15**, 1085 (1985).
8. More correctly Ekman pumping involves a combination of both the zonal wind stress and the curl of the wind stress. The curl of the horizontal wind can be visualized as the rate of rotation of a vertical axis paddle wheel at a given location.
9. W. B. White *et al.*, *J. Phys. Oceanogr.* **15**, 917 (1985).
10. J. S. Godfrey, *ibid.* **5**, 399 (1975).
11. K. Wyrski, *J. Geophys. Res.* **90**, 7129 (1985).
12. J. P. McCreary, *Mon. Weather Rev.* **111**, 370 (1983).
13. H. E. Hurlbert *et al.*, *J. Phys. Oceanogr.* **6**, 621 (1976); J. P. McCreary, *ibid.*, p. 632; M. Cane and E. S. Sarachik, *J. Marine Res.* **35**, 395 (1977).
14. B. Hickey, *J. Phys. Oceanogr.* **5**, 475 (1975).
15. S. G. H. Philander *et al.*, *J. Atmos. Sci.* **41**, 604 (1984).
16. G. K. Vallis, *Science* **232**, 243 (1986).
17. P. S. Schopf and M. Suarez, *J. Atmos. Sci.* **45**, 549 (1988).
18. M. A. Cane and S. E. Zebiak, *Science* **228**, 1085 (1985); S. E. Zebiak, *Mon. Weather Rev.* **114**, 1263 (1986); M. A. Cane *et al.*, *Nature* **321**, 827 (1986); S. E. Zebiak and M. A. Cane, *Mon. Weather Rev.* **115**, 2262 (1987).
19. T. P. Barnett *et al.*, *Science*, in press.
20. D. S. Battisti, unpublished results.
21. N. E. Graham *et al.*, *J. Geophys. Res.* **92**, 14271 (1987).
22. M. A. Cane, *J. Phys. Oceanogr.* **14**, 1864 (1984).
23. E. M. Rasmusson and T. H. Carpenter, *Mon. Weather Rev.* **110**, 354 (1982).
24. A. J. Busalacchi and J. J. O’Brien, *J. Phys. Oceanogr.* **10**, 1929 (1980); *J. Geophys. Res.* **86**, 10901 (1981); A. J. Busalacchi *et al.*, *ibid.* **88**, 7551 (1983).
25. A. J. Busalacchi and M. A. Cane, *J. Phys. Oceanogr.* **15**, 213 (1985).
26. W. B. White *et al.*, *ibid.* **17**, 264 (1987).
27. The starting point is, of course, arbitrary; some initial disturbance or imbalance is assumed to start the oscillations.
28. N. E. Graham *et al.*, *J. Geophys. Res.* **92**, 14251 (1987).
29. T. P. Barnett, *Mon. Weather Rev.* **112**, 1403 (1984).
30. A. E. Gill, *Q. J. R. Meteorol. Soc.* **106**, 447 (1980); R. N. Keshavamurty, *J. Atmos. Sci.* **39**, 1241 (1982); M. I. Blackmon *et al.*, *ibid.* **40**, 1410 (1983); J. Shukla and J. M. Wallace, *ibid.*, p. 1613; M. J. Fennessey *et al.*, *Mon. Weather Rev.* **113**, 858 (1985); N. C. Lau, *ibid.*, p. 1970.
31. G. Cornejo-Garrido and P. H. Stone, *J. Atmos. Sci.* **34**, 1155 (1977); J. D. Neelin and I. M. Held, *Mon. Weather Rev.* **115**, 3 (1987).
32. N. E. Graham and T. P. Barnett, *Science* **238**, 657 (1987).
33. S. B. Goldenberg and J. J. O’Brien, *Mon. Weather Rev.* **109**, 1190 (1981).
34. T. P. Barnett and R. Preisendorfer, *ibid.* **115**, 1825 (1987).
35. These SST and wind stress data patterns evolve during warm and cool phases of the ENSO cycle. At other times of the year the major westerly wind anomalies in the western Pacific are centered south of the equator [see (23, 28)].
36. M. A. Cane, *J. Marine Res.* **37**, 253 (1979).
37. R. Cheney *et al.*, *Johns Hopkins APL Tech. Dig.* **8**, 245 (1987).
38. G. Meyers, *J. Phys. Oceanogr.* **12**, 1161 (1982).

39. S. E. Pazan *et al.*, *J. Geophys. Res.* **91**, 8437 (1986).
 40. M. Inoue and J. J. O'Brien, *ibid.* **92**, 5045 (1987).
 41. M. Inoue *et al.*, *ibid.*, p. 11671.
 42. T. P. Barnett and K. Hasselmann, *Rev. Geophys. Space Phys.* **17**, 949 (1979); K.-M. Lau and P. H. Chan, *Mon. Weather Rev.* **113**, 1889 (1985).
 43. The first mode (14% of the variance) centers on a trend of rising sea level at most locations, particularly Legaspi (Philippines), Callao (Peru), and Honolulu.
 44. This value is a fixed parameter in the Florida State University ocean model but one that can be estimated from oceanographic data.
 45. T. P. Barnett, *Mon. Weather Rev.* **112**, 2380 (1984); *J. Atmos. Sci.* **42**, 478 (1985); A. E. Gill and E. M. Rasmusson, *Nature* **306**, 229 (1983); R. S. Quiroz, *Mon. Weather Rev.* **111**, 1685 (1983).
 46. The relation for off-equatorial ULT represents an implicit integration of Ekman pumping through time for one time step only. A more reasonable approach, where the effects of current and past forcing are both included to simulate the fact that off-equatorial Rossby wave activity represents an accumulation of forcing, does not change the results substantially.
 47. Both T_{av} and FSU model ULT data show that the largest ULT anomalies associated with ENSO in the North Pacific are located between 12° and 16° latitude and require 1 to 2 years to propagate from the central Pacific to the maritime coast of Asia.
 48. For example, "40 to 60" day oscillations [R. A. Madden and P. R. Julian, *J. Atmos. Sci.* **28**, 702 (1971)] and "west wind bursts" [D. S. Luther, D. E. Harrison, R. A. Knox, *Science* **222**, 327 (1983); K.-M. Lau and M.-T. Li, *Bull. Am. Meteorol. Soc.* **65**, 114 (1985)].
 49. G. K. Vallis, *J. Geophys. Res.*, in press.
 50. The authors are grateful to T. Barnett, M. Cane, D. Cayan, J. O'Brien, G. Vallis, and K. Wyrki for discussions and useful suggestions. The comments of two anonymous reviewers were also helpful. The integrations of the FSU ocean model were performed by M. Kubota; these data were kindly provided by V. Panchang and J. O'Brien. This work was funded in part by National Science Foundation under grants ATM85-13713 and OCE86-07962.

DNA Damage and Oxygen Radical Toxicity

JAMES A. IMLAY* AND STUART LINN

A major portion of the toxicity of hydrogen peroxide in *Escherichia coli* is attributed to DNA damage mediated by a Fenton reaction that generates active forms of hydroxyl radicals from hydrogen peroxide, DNA-bound iron, and a constant source of reducing equivalents. Kinetic peculiarities of DNA damage production by hydrogen peroxide in vivo can be reproduced by including DNA in an in vitro Fenton reaction system in which iron catalyzes the univalent reduction of hydrogen peroxide by the reduced form of nicotinamide adenine dinucleotide (NADH). To minimize the toxicity of oxygen radicals, the cell utilizes scavengers of these radicals and DNA repair enzymes. On the basis of observations with the model system, it is proposed that the cell may also decrease such toxicity by diminishing available NAD(P)H and by utilizing oxygen itself to scavenge active free radicals into superoxide, which is then destroyed by superoxide dismutase.

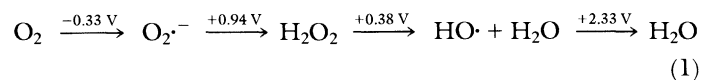
THE APPEARANCE OF ATMOSPHERIC OXYGEN OFFERED TO the evolving biota the opportunity to utilize molecular oxygen as the terminal oxidant in respiration in order to gain energetic advantages over fermentation and respiratory pathways that rely on other oxidants. However, the presence of intracellular oxygen also allowed inadvertent redox reactions by oxygen radicals to damage critical biomolecules, and a variety of human disease states, including atherosclerosis, cancer, and aging have been attributed to such damage (1). This article describes the chemistry by which one oxidant, hydrogen peroxide (H₂O₂), generates toxic lesions in DNA and how the cell protects itself against such lesions.

Sources of Oxidative Stress

A variety of external oxidative stresses have toxic consequences in bacterial and eukaryotic cells. Hyperbaric oxygen, gamma radiation,

near-ultraviolet (near-UV) radiation, ozone, peroxides, and redox-cycling drugs all exert deleterious effects through the intermediacy of oxygen species. We selected H₂O₂ for study of such phenomena because of the likelihood that it is central to the cytotoxic action of many of these agents and because the routine generation of H₂O₂ as a by-product of oxidative metabolism might cause it also to be an important endogenous oxidant in aerobic organisms. *Escherichia coli* was selected as an experimental organism because of its simple growth requirements, its ability to grow anaerobically or aerobically, and the extensive knowledge available concerning its genetics and enzymology.

Although molecular oxygen is strongly oxidative with respect to its fully reduced form, water, its oxidative potential is normally held in check by kinetic restrictions that are imposed by its two unpaired, spin-parallel electrons. However, consecutive univalent reductions of oxygen produce superoxide (O₂⁻), H₂O₂, and hydroxyl radical (HO·), with the reaction potentials shown:



Each of these is exempt from the spin restriction and is kinetically and thermodynamically proficient at monovalent electron exchanges. The O₂⁻ is notable in that it can act either as an oxidant or a reductant. Hydrogen peroxide is a relatively stable oxidant, but the HO· is an extremely powerful oxidant that reacts at nearly diffusion-limited rates with most organic substrates. The relatively mild oxidative capabilities of O₂⁻ and H₂O₂ belie the severity of their direct oxidative effects on biomolecules; therefore, it has been assumed that their cytotoxic nature might be due to their ability to generate intracellular HO·.

Stuart Linn is a professor of biochemistry at University of California, Berkeley, and James A. Imlay is currently a Jane Coffin Childs Postdoctoral Fellow at Duke University.

*Present address: Department of Biochemistry, Duke University Medical Center, Durham, NC 27710